

# Competing Interactions in Low-Dimensional Spin 1/2 Systems

Helge Rosner, Miriam Schmitt, Oleg Janson, Alexander Tsirlin<sup>1</sup>, Deepa Kasinathan, Ulrike Nitzsche<sup>2</sup>, Klaus Koepernik<sup>2</sup>, Sylvia Golbs, Markus Schmidt, and Walter Schnelle

## Introduction

Low-dimensional spin systems are very actively studied subjects in solid state physics, since they allow for the observation of numerous quantum phenomena and to interpret these phenomena within relatively simple models, e.g., Ising or Heisenberg. An interesting phenomenon in spin physics is the formation of a spin liquid – a strongly correlated ground state lacking long range magnetic order. This ground state is usually related to the electronic mechanism of superconductivity suggested for high- $T_c$  cuprates. Spin liquids originate from quantum fluctuations that are particularly strong in systems with reduced dimensionality and low spin value. The fluctuations can be further enhanced by introducing magnetic frustration which impedes long-range ordering of the system due to a high degree of degeneracy.

On the other hand, many systems tend to avoid degenerate ground states, for instance by lattice distortion, orbital ordering or a combination of both. In our study, we present these phenomena – caused by competing interactions – for selected systems with a square lattice of spin 1/2 transition-metal cations.

## Frustrated Square Lattice Systems

The spin-1/2 frustrated square lattice (FSL) is one of the simplest models giving rise to a spin liquid ground state. In this model, also known as the  $J_1$ - $J_2$  model, magnetic moments on a square lattice are subjected to nearest-neighbor interaction  $J_1$  along the side of the square and next-nearest neighbor interaction  $J_2$  along the diagonal of the square (see Fig. 1). The FSL model is described by the frustration ratio  $\alpha = J_2/J_1$  (Fig. 1 and Ref. [1]). Extensive theoretical research on the FSL model has been performed in the past. Initially, the studies were focused on the antiferromagnetic (AFM) region  $J_1, J_2 > 0$  [5] while the general case – arbitrary signs for  $J_1$  and  $J_2$  – was only considered quite recently [1]. The phase diagram of the model

(Fig. 1) includes three regions with different ordered phases: ferromagnet (FM,  $Q = (0,0)$ ), Néel antiferromagnet (NAF,  $Q = (\pi,\pi)$ ), and columnar antiferromagnet (CAF,  $Q = (0,\pi)$  or  $(\pi,0)$ ). Classically, first-order phase transitions should occur at the NAF-CAF ( $\alpha = 0.5$ ) and the CAF-FM ( $\alpha = -0.5$ ) boundaries. However, quantum fluctuations destroy long-range ordering and cause the formation of critical regions with disordered ground states. In general, the ground state in the critical regions is referred to as a quantum spin-liquid regime, but the particular nature of the spin-liquid phase is still under discussion.

Despite numerous theoretical investigations, experimental realizations of the  $J_1$ - $J_2$  model are scarce. Layered vanadium oxides  $\text{Li}_2\text{VOXO}_4$  ( $X = \text{Si, Ge}$ ) were the first examples of the FSL systems. Initially, these materials were ascribed close to the critical region ( $\alpha \sim 1$ ) of the phase diagram [6,7]. However, later studies established a different scenario for these systems, indicating that the  $\text{Li}_2\text{VOXO}_4$  compounds fall deep into the CAF region with  $\alpha \gg 1$  [8,9,10]. No compound close to the critical region  $\alpha = 0.5$  had been reported thus far.

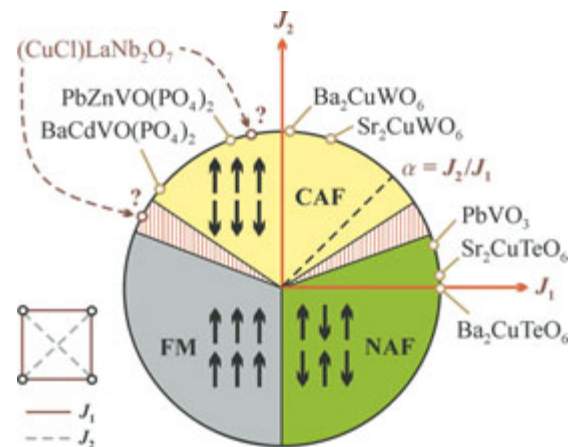


Fig. 1: Phase diagram of the FSL model (see also [2]). Solid filling indicates the regions of long-range magnetic ordering (CAF, FM, NAF, see text), hatched filling denotes the critical regions. The positions of the compounds discussed in the text are marked together with those of the closely related compounds  $\text{BaCdVO}(\text{PO}_4)_2$  [3] and  $\text{PbZnVO}(\text{PO}_4)_2$  [4].

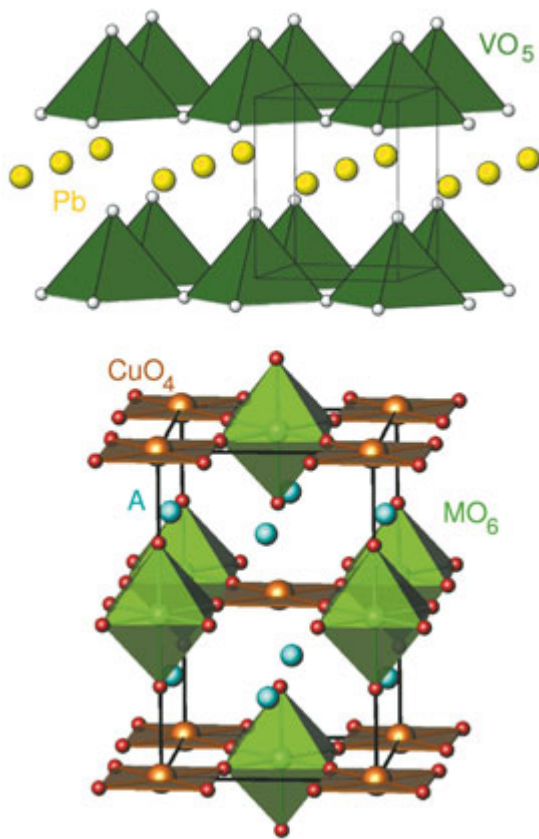


Fig. 2: Crystal structures of  $\text{PbVO}_3$  (top) and the FSL model compounds  $A_2\text{CuMO}_6$  ( $A = \text{Sr}, \text{Ba}$ ;  $M = \text{Te}, \text{W}$ ) (bottom). The magnetic  $\text{CuO}_4$  and  $\text{VO}_5$  units are indicated by the orange squares and green pyramids, respectively. The  $\text{MO}_6$  octahedra in  $A_2\text{CuMO}_6$  are shown in green, the other cations are indicated by spheres.

Below, we present magnetic properties of the novel compound  $\text{PbVO}_3$  [11] that exhibits a spin-1/2 FSL. Our experimental and computational studies show that this compound lies close to the critical region of FSL and does not undergo long-range magnetic ordering down to 1.8 K [12].  $\text{PbVO}_3$  adopts a layered perovskite-type structure shown in Fig. 2. The structure combines the absence of an inversion center with a magnetic  $V^{4+}$  cation; therefore,  $\text{PbVO}_3$  also attracts considerable attention as a possible multiferroic material.

Polycrystalline samples of  $\text{PbVO}_3$  were prepared by a high-temperature high-pressure technique and investigated via susceptibility and specific heat measurements. To evaluate the leading exchange couplings, the susceptibility data were fitted using the high-temperature series expansion (HTSE) for the FSL [9], resulting in  $J_1 \sim 190\text{K}$  and a ratio  $\alpha = J_2/J_1 = 0.38$  in close vicinity to the critical

region. This finding is consistent with the specific heat measurements that show no indication of magnetic ordering down to 1.8 K.

Since experimental data for the current sample material provide only limited microscopic insight into the magnetic properties of  $\text{PbVO}_3$ , we further support our study using computational techniques. Band structure calculations are known to be a useful tool to estimate exchange integrals and understand the properties of low-dimensional spin systems [8]. Scalar relativistic band structure calculations were performed using the full-potential local-orbital scheme (FPLO) [13]. Combining a tight-binding (TB) model approach and the LSDA+ $U$  technique, we find  $J_1 = 200\text{K}$  and  $\alpha = 0.2 \dots 0.3$  in good agreement with the experimental results.

The applied techniques are demonstrated in more detail for another novel FSL compound family  $A_2\text{CuMO}_6$  ( $A = \text{Sr}, \text{Ba}$ ;  $M = \text{Te}, \text{W}$ ). The compounds have a tetragonal crystal structure (see Fig. 2) with isolated, planar  $\text{CuO}_4$  plaquettes interlinked to a two-dimensional network by  $\text{MO}_6$  octahedrons. The results of FPLO band structure calculations within the local density approximation (LDA) are shown in Fig. 3. An analysis of the electronic density of states (DOS) reveals that the magnetically relevant orbitals at the Fermi level originate predominantly from the Cu-O plaquette states of  $x^2-y^2$  symmetry. The metallic behavior is a well known LDA shortcoming due to the underestimation of the electron correlations in this approximation. The correlations can be taken into

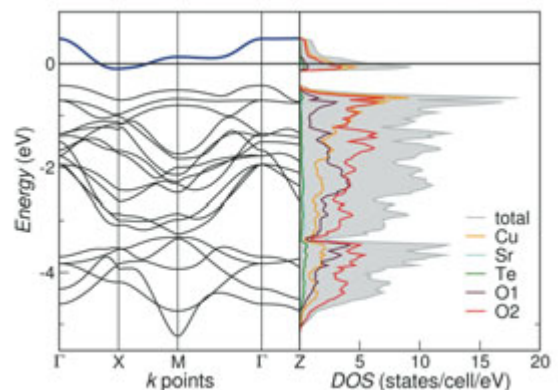


Fig. 3: Calculated band structure (left panel) as well as total and partial electronic density of states (right panel) for the compound  $\text{Sr}_2\text{CuTeO}_6$ . The antibonding band relevant for the magnetism (shown in blue) originates predominantly from Cu-O plaquette states.

account by mapping a TB model for the relevant band (see Fig. 3) via a Hubbard model onto a Heisenberg model. This band exhibits dispersion in the tetragonal plane only, indicating a pronounced two-dimensional character. The TB fit and the subsequent mapping reveal that the compounds with  $M=W$  fall into the CAF region ( $\alpha \gg 1$ ), whereas the  $M=Te$  systems belong to the NAF region ( $\alpha \ll 1$ ) like most of the undoped high temperature superconducting compounds (Fig. 1). Alternatively, the strong correlations can be taken into account explicitly in the band structure calculations within the LSDA+ $U$  approach. In good agreement with the TB-based results, these calculations confirm the assigned positions in the phase diagram.

For all four compounds, polycrystalline samples were prepared and susceptibility measurements have been carried out (Fig. 4). All susceptibility curves show a pronounced maximum that is characteristic for low-dimensional spin systems. To evaluate the magnetic couplings, the data can be fitted using the FSL HTSE. Due to an internal symmetry of the FSL Hamiltonian, the solutions for these fits are ambiguous, but one of the two solutions can be excluded in comparison with the calculational results. The other solution (Fig. 4) yields excellent agreement with the theoretical estimates for all four systems [14].

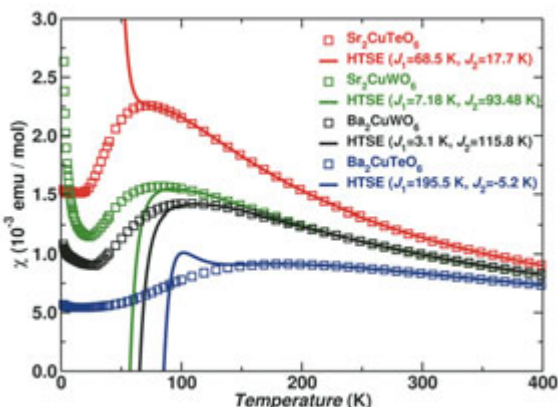


Fig. 4: Measured susceptibility (colored squares) for the  $A_2CuMO_6$  compounds together with numeric fits (full lines) of the HTSE for the  $J_1$ - $J_2$  model. The values for the resulting exchange parameters are given in the legend.

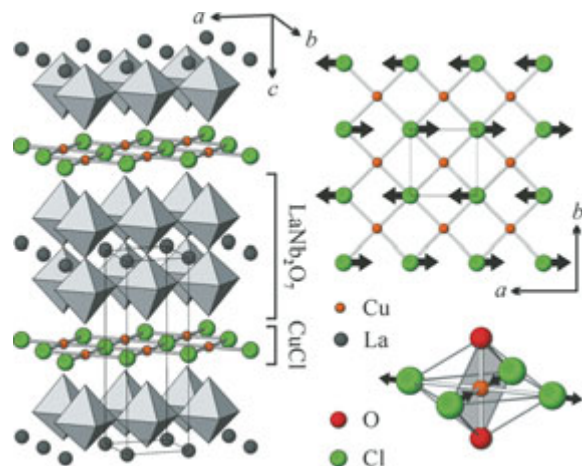


Fig. 5: Regular (tetragonal) crystal structure of  $(CuCl)LaNb_2O_7$ : stacking of perovskite-type  $[LaNb_2O_7]$  blocks and rocksalt-type  $[CuCl]$  layers (left panel), the single  $[CuCl]$  layer (upper right panel), and the  $CuO_2Cl_4$  squeezed octahedron (bottom right panel). The regular structure of the  $[CuCl]$  layer gives rise to the frustrated  $J_1$ - $J_2$  square lattice model, the structural distortion indicated by arrows leads to a quasi one-dimensional model with frustrating inter-chain couplings.

## Magnetic Order Ruled by Orbital Order

### $(CuCl)LaNb_2O_7$

Initially, the compound  $(CuCl)LaNb_2O_7$  was also considered as a realization of the FSL model. According to Ref. [15] the compound exhibits a layered tetragonal crystal structure (Fig. 5).  $(CuCl)LaNb_2O_7$  exhibits quite low Curie-Weiss temperature  $\theta_{CW}$  of about 10 K and a spin gap  $\Delta \sim 26$  K [16]. These data are inconsistent with the FSL model and with the results of our band structure calculations for the tetragonal structure, yielding exchange interactions that exceed the measured  $\theta_{CW}$  by more than an order of magnitude.

A closer inspection of the calculated DOS based on the tetragonal crystal structure (Fig. 5) reveals an unusual occupation of the Cu  $3d_{3z^2-r^2}$  orbital and a resulting competition of two different orbital states. Therefore, we challenged the structural stability of the compound computationally, since lattice distortion towards a lower symmetry could lift the above mentioned near-degeneracy. Our total energy calculations provide strong indication for a structural distortion from a re-organization of the Cl atoms in the Cu-Cl plane (Fig. 5). The distortion leads to a reorientation of the magnetically active orbital and, in turn, to a completely different magnetic coupling regime. Instead of a two-dimensional FSL model we suggest a quasi one-



dimensional scenario of chains that exhibit sizeable frustrating inter-chain interactions [17]. Due to the new orientation of the magnetically active orbital (Fig. 5), the leading exchange integral is reduced by almost an order of magnitude and is now in line with the measured  $\theta_{CW}$ . Our suggested distortion scenario is consistent with recent NMR measurements and neutron as well as electron diffraction data [16,18,19].

### CuSb<sub>2</sub>O<sub>6</sub>

Another closely related compound with respect to competing ground-state orbitals is the system CuSb<sub>2</sub>O<sub>6</sub>. Although the system exhibits a tetragonal crystal structure [20] (Fig. 6), susceptibility [21] and neutron data [22] exhibit very pronounced one-dimensional magnetism that can be well described by a nearest neighbor Heisenberg chain with an exchange of about 100 K. To investigate its microscopic origin, we carried out band structure calculation and analyzed the resulting band structure and orbital occupation [23]. Similar to (CuCl)LaNb<sub>2</sub>O<sub>7</sub> and unlike the standard cuprate scenario, we find the  $3d_{x^2-y^2}$  and  $3d_{3z^2-r^2}$  derived states at the Fermi level. A TB analysis of both band complexes reveals that a half-filled, magnetically active orbital of  $3z^2-r^2$  symmetry is consistent with the observed one-dimensionality, whereas the  $3d_{x^2-y^2}$  states would lead to a three-dimensional model with exchange constants of a few Kelvin conflicting the experimental results.

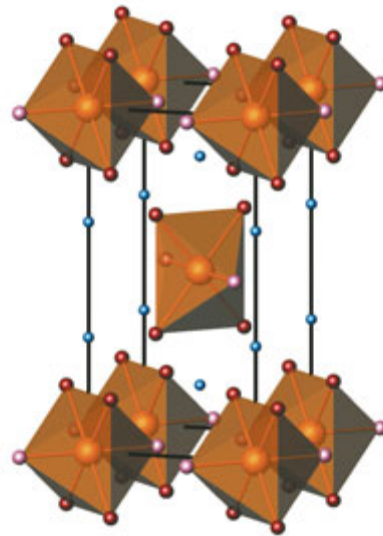


Fig. 6: Tetragonal crystal structure of CuSb<sub>2</sub>O<sub>6</sub>. The almost regular CuO<sub>6</sub> octahedra are colored in orange, the two crystallographic O sites in different shades of red, and Sb is presented by blue spheres.

Our subsequent LSDA+*U* calculations fully support the picture derived from the TB analysis. The strong electron correlations drive the system to an orbitally ordered (OO) ground state of  $3d_{3z^2-r^2}$  symmetry (Fig. 7) which is energetically favored by about 110 meV compared to the  $3d_{x^2-y^2}$  state. The OO model obtains further confirmation from the calculation of the corresponding nearest neighbor coupling. We find an exchange constant of 140 K in good agreement with the measured

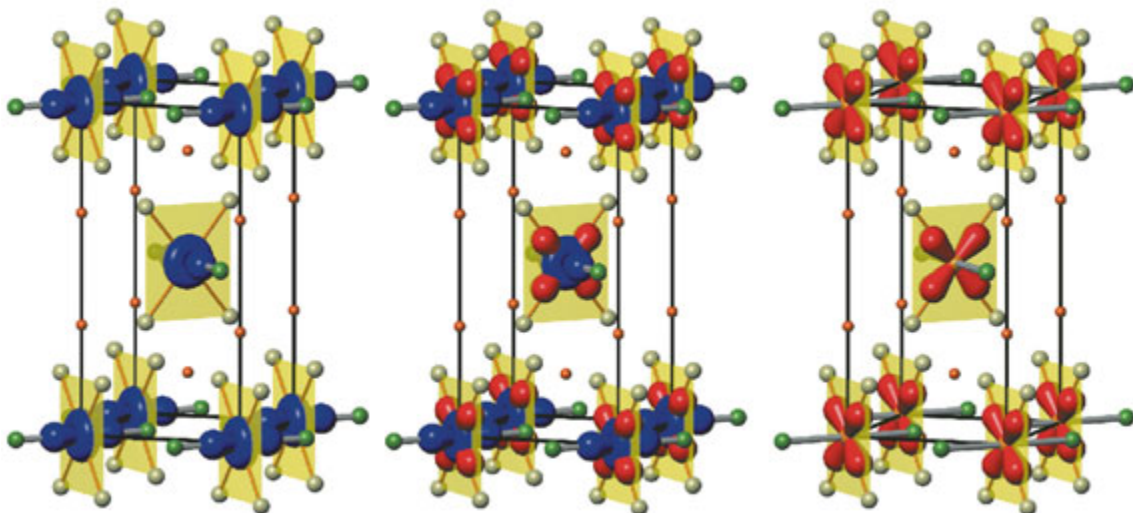


Fig. 7: Middle panel: The competition of in-plaquette and out-of-plaquette orbitals in LDA for CuSb<sub>2</sub>O<sub>6</sub>. Both orbitals are partially occupied and comprise the Fermi surface. Right panel: Standard picture of high  $T_c$  cuprates with the inclusion of strong Coulomb correlations *U*. The plaquette orbitals remain half-filled and thereby would lead to 3D magnetic order. Left panel: Unique orbital ordering in CuSb<sub>2</sub>O<sub>6</sub> leading to a pronounced one-dimensional magnetic behavior.

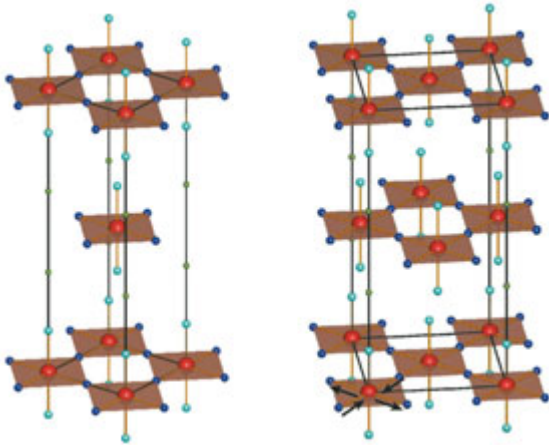


Fig. 8: Tetragonal (left panel) and orthorhombic (right panel) crystal structure of  $\text{Cs}_2\text{AgF}_4$ . The original  $\text{AgF}_4$  plaquettes with Ag (red sphere) in the center and F at the corner (blue) are shown in brown. A distortion of the F sublattice, indicated by arrows, leads to orthorhombic symmetry with a pseudo-tetragonal lattice.

value of about 100 K [21]. Further experiments using X-ray absorption spectroscopy and electron spin resonance measurements on single crystals to confirm the peculiar OO of  $\text{CuSb}_2\text{O}_6$  more directly are under way.

### $\text{Cs}_2\text{AgF}_4$

Finally, we studied the square lattice compound  $\text{Cs}_2\text{AgF}_4$  where the combination of distortion and strong correlation drive an OO ground state that surprisingly leads to a FM order. The originally published tetragonal crystal structure of  $\text{Cs}_2\text{AgF}_4$  [24] is shown in Fig. 8. Recently, inelastic neutron measurements revealed an OO ground state for this compound [25] (Fig. 9) that is inconsistent with the tetragonal symmetry. A new refinement of the crystal structure from neutron data resulted in a distortion of the F partial structure (Fig. 8), reducing the symmetry to orthorhombic with almost identical in-plane lattice parameters. On the other hand, the new refinement did not provide a significant improvement of the corresponding reliability factor  $R$ .

Our band structure calculations for both the tetragonal and the orthorhombic symmetry reveal an interesting interplay of distortion and strong electron correlation that fully describes the observed OO FM ground state [26]. As for the previous compounds, LDA calculations result in a competition of orbitals with  $x^2-y^2$  and  $3z^2-r^2$  symmetry. The distortion of the F partial structure, however,

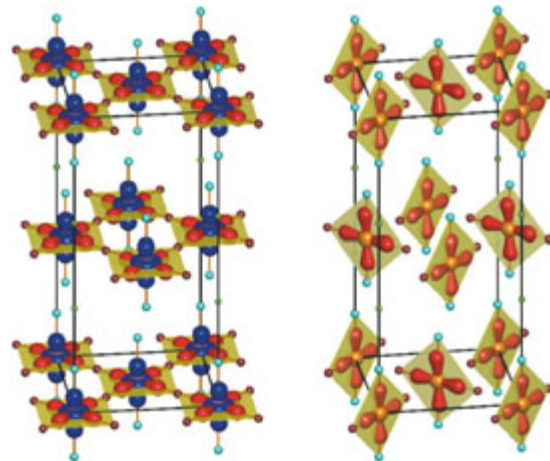


Fig. 9: Left panel: Itinerant scenario for the tetragonal  $\text{Cs}_2\text{AgF}_4$  with both  $e_g$  orbitals partially occupied. Right panel: Orbitally ordered scenario wherein the distortions along with the exchange lower one of the  $e_g$  orbitals, leaving half filled only the plaquette orbitals shown.

is energetically favored even neglecting the strong correlations. On the other hand, the corresponding energy gain would be far too small to explain the stability of this distortion at room temperature. In addition, without an explicit treatment of the Coulomb repulsion the ground state should be dominated by AFM exchange. Including the correlations in the LSDA+ $U$  approach results in a large energy gain for the OO state (Fig. 9) of about 200 meV (corresponding to about 2300 K). The resulting exchange coupling of  $-4.5$  meV is in perfect agreement with the experimental findings of  $-3.8$  to  $-5$  meV. Thus, our study indicates that, the peculiar interplay of lattice distortion and strong correlation is crucial to understand the OO FM ground state in  $\text{Cs}_2\text{AgF}_4$ .

### Conclusion

In our study we have demonstrated that low dimensional spin 1/2 systems can exhibit a large variety of magnetic ground states, even if the underlying crystal lattice is the same. This different behavior is generated by a complex interplay of magnetic, orbital and lattice degrees of freedom. To elucidate this complex situation, the combination of theoretical electronic structure calculations, thermodynamic and spectroscopic measurements is a very powerful tool for a deep microscopic understanding.

## References

- [1] *N. Shannon, B. Schmidt, K. Penc, and P. Thalmeier*, *Eur. Phys. J. B* **38** (2004) 599.
- [2] *B. Schmidt, P. Thalmeier, and N. Shannon*, *Phys. Rev. B* **76** (2007) 125113.
- [3] *R. Nath, A. A. Tsirlin, H. Rosner, and C. Geibel*, *Phys. Rev. B* **78** (2008) 064422.
- [4] *A. A. Tsirlin, R. Nath, C. Geibel, R. V. Shpanchenko, E. V. Antipov, and H. Rosner*, in preparation.
- [5] *P. Chandra and B. Doucot*, *Phys. Rev. B* **38** (1988) 9335.
- [6] *R. Melzi, P. Carretta, A. Lascialfari, M. Mambri, M. Troyer, P. Millet, and F. Mila*, *Phys. Rev. Lett.* **85** (2000) 1318.
- [7] *R. Melzi, S. Aldrovandi, F. Tedoldi, P. Carretta, P. Millet, and F. Mila*, *Phys. Rev. B* **64** (2001) 024409.
- [8] *H. Rosner, R.R.P. Singh, W.H. Zheng, J. Oitmaa, S.-L. Drechsler, and W. E. Pickett*, *Phys. Rev. Lett.* **88** (2002) 186405.
- [9] *H. Rosner, R.R.P. Singh, W.H. Zheng, J. Oitmaa, and W. E. Pickett*, *Phys. Rev. B* **67** (2003) 014416.
- [10] *A. Bombardi, J. Rodriguez-Carvajal, S. Di Matteo, F. de Bergevin, L. Paolasini, P. Carretta, P. Millet, and R. Caciuffo*, *Phys. Rev. Lett.* **93** (2004) 027202.
- [11] *R. V. Shpanchenko, V. V. Chernaya, A. A. Tsirlin, P. S. Chizhov, D. E. Sklovsky, and E. V. Antipov*, *Chem. Mater.* **16** (2004) 3267.
- [12] *A. A. Tsirlin, A. A. Belik, R. V. Shpanchenko, E. V. Antipov, E. Takayama-Muromachi, and H. Rosner*, *Phys. Rev. B* **77** (2008) 092402.
- [13] *K. Koepernik, and H. Eschrig*, *Phys. Rev. B* **59** (1999) 1743.
- [14] *M. Schmitt, O. Janson, M. Schmidt, W. Schnelle and H. Rosner*, in preparation.
- [15] *T. A. Kodenkandath, J. N. Lalena, W. L. Zhou, E. E. Carpenter, C. Sangregorio, A. U. Falster, W. B. Simmons Jr., C. J. O'Connor, and J. B. Wiley*, *J. Amer. Chem. Soc.* **121** (1999) 10743.
- [16] *H. Kageyama, T. Kitano, N. Oba, M. Nishi, S. Nagai, K. Hirota, L. Viciu, J. B. Wiley, J. Yasuda, Y. Baba, et al.*, *J. Phys. Soc. Jpn.* **74** (2005) 1702.
- [17] *A. A. Tsirlin, and H. Rosner*, *arxiv:0901.0154* (submitted to PRB).
- [18] *G. Caruntu, T. A. Kodenkandath, and J. B. Wiley*, *Mater. Res. Bull.* **37** (2002) 593.
- [19] *M. Yoshida, N. Ogata, M. Takigawa, J. Yamaura, M. Ichihara, T. Kitano, H. Kageyama, Y. Ajiro, and K. Yoshimura*, *J. Phys. Soc. Jpn.* **76** (2007) 104703.
- [20] *E.-O. Giere, A. Brahim, H. J. Deiseroth, and D. Reinen*, *J. Solid State Chem.* **131** (1997) 263.
- [21] *A. M. Nakua, and J. E. Greedan*, *J. Solid State Chem.* **188** (1995) 199.
- [22] *B. J. Gibson, R. K. Kremer, A. V. Prokofiev, W. Assmus, B. Ouladdiaf*, *J. Mag. Mag. Mater.* **272-276** (2004) 927.
- [23] *D. Kasinathan, K. Koepernik, and H. Rosner*, *Phys. Rev. Lett.* **199** (2008) 237202.
- [24] *R.-H. Odenthal, D. Paul, and R. Hoppe*, *Z. Anorg. Allg. Chem.* **407** (1974) 144.
- [25] *S. E. McLain, M. R. Dolgos, D. A. Tennant, J. F. C. Turner, T. Barnes, T. Proffen, B. C. Sales and R. I. Bewley*, *Nature Materials* **5** (2006) 561.
- [26] *D. Kasinathan, K. Koepernik, U. Nitzsche, and H. Rosner*, *Phys. Rev. Lett.* **99** (2007) 247210.

<sup>1</sup> in cooperation with Department of Chemistry, Moscow State University, Moscow, Russia

<sup>2</sup> IFW Dresden, Germany